COMPUTED TOMOGRAPHY OF THE BODY

With Magnetic Resonance Imaging

Volume Three
Abdomen and Pelvis

COMPUTED TOMOGRAPHY OF THE BODY

With Magnetic Resonance Imaging

Second Edition

Albert A. Moss, M.D.
Professor and Chairman, Department of Radiology
University of Washington School of Medicine
Seattle, Washington

Gordon Gamsu, M.D.
Professor of Radiology and Medicine
University of California, San Francisco, School of Medicine
San Francisco, California

Harry K. Genant, M.D.
Professor of Radiology, Medicine, and Orthopaedic Surgery; Chief of the Musculoskeletal Section; Director of the Osteoporosis Research Group
University of California, San Francisco, School of Medicine
San Francisco, California

Volume Three
Abdomen and Pelvis

W.B. SAUNDERS COMPANY
Harcourt Brace Jovanovich, Inc.
Philadelphia London Toronto Montreal Sydney Tokyo

W. B. SAUNDERS COMPANY
Harcourt Brace Jovanovich, Inc.

The Curtis Center
Independence Square West
Philadelphia, Pennsylvania 19106

Library of Congress Cataloging-in-Publication Data

Moss, Albert A.

Computed tomography of the body with magnetic resonance imaging / Albert A. Moss, Gordon Gamsu, Harry K. Genant. — 2nd ed.

p. cm.

Rev. ed. of: Computed tomography of the body / Albert A. Moss, Gordon Gamsu, Harry K. Genant.

Includes bibliographical references and index.

ISBN 0-7216-2415-4 (set)

1. Tomography. 2. Magnetic resonance imaging.
I. Gamsu, Gordon. II. Genant, Harry K.
III. Moss, Albert A. Computed tomography of the body.
IV. Title.

[DNLM: 1. Anatomy, Regional. 2. Magnetic Resonance Imaging. 3. Tomography, X-Ray Computed. WN 160 M913c]

RC78.7.T6M68 1992

DNLM/DLC 91-32837

Editor: Lisette Bralow
Designer: W.B. Saunders Staff
Production Manager: Peter Faber
Manuscript Editors: Lorraine Zawodny and Kendall Sterling
Illustration Coordinator: Walter Verbitski
Indexer: Nancy Newman
Cover Designer: Michelle Maloney

Computed Tomography of the Body With Magnetic Resonance Imaging, 2/e.

ISBN Volume I 0-7216-4358-2
Volume II 0-7216-4359-0
Volume III 0-7216-4503-8
Three Volume Set 0-7216-2415-4

Printed in the United States of America

Last digit is the print number: 9 8 7 6 5 4 3 2 1

CONTRIBUTORS FOR VOLUME THREE

RICHARD L. BARON, M.D.
Professor, Department of Radiology, University of Pittsburgh School of Medicine; Director, Body CT/MRI; Co-Director, Abdominal Imaging, Presbyterian-University Hospital; Pittsburgh, PA
THE BILIARY TRACT
THE LIVER

DOUGLAS P. BOYD, Ph.D.
Adjunct Professor of Radiology, University of California, San Francisco, School of Medicine; Chairman of the Board, Imatron, Inc.; San Francisco, CA
PRINCIPLES OF COMPUTED TOMOGRAPHY

DAVID K. BREWER, M.D.
Associate Professor of Radiology, Adjunct Assistant Professor of Pediatrics, University of Washington School of Medicine; Children's Hospital and Medical Center; Seattle, WA
PEDIATRIC BODY IMAGING

WILLIAM H. BUSH, M.D.
Professor of Radiology, Chief, Uroradiology, Department of Radiology, University of Washington School of Medicine, Seattle, WA
THE KIDNEYS

PETER L. DAVIS, M.D.
Associate Professor, Department of Radiology, University of Pittsburgh School of Medicine; Research Administrator, Pittsburgh NMR Institute; Pittsburgh, PA
PRINCIPLES OF MAGNETIC RESONANCE IMAGING

MICHAEL P. FEDERLE, M.D.
Professor and Chairman, Department of Radiology, University of Pittsburgh School of Medicine; Attending Staff, Presbyterian-University Hospital; Pittsburgh, PA
THE PANCREAS
THE SPLEEN

PATRICK C. FREENY, M.D.
Professor of Radiology and Director of Abdominal Imaging, University of Washington School of Medicine, Seattle, WA
THE LIVER

HENRY I. GOLDBERG, M.D.
Professor, Department of Radiology, University of California, San Francisco, School of Medicine, San Francisco, CA
THE PANCREAS

MITCHELL M. GOODSITT, Ph.D.
Assistant Professor of Radiology (Physics); Adjunct Assistant Professor of Radiological Sciences; Adjunct Assistant Professor of Bioengineering; University of Washington School of Medicine; Director, Diagnostic Physics, Department of Radiology, University of Washington Medical Center, Seattle, WA
PRINCIPLES OF COMPUTED TOMOGRAPHY

R. BROOKE JEFFREY, JR., M.D.
Professor of Radiology, Stanford University School of Medicine; Chief of Abdominal Imaging, Department of Diagnostic Radiology and Nuclear Medicine, Stanford University Medical Center; Stanford, CA
THE RETROPERITONEUM AND LYMPHOVASCULAR STRUCTURES
THE PERITONEAL CAVITY AND MESENTERY

SHIRLEY M. McCARTHY, M.D., Ph.D.
Associate Professor, Diagnostic Radiology, Yale School of Medicine; Director, Magnetic Resonance Imaging, Yale New Haven Hospital; New Haven, CT
THE PELVIS

ALBERT A. MOSS, M.D.
Professor and Chairman, Department of Radiology, University of Washington School of Medicine, Seattle, WA
THE GASTROINTESTINAL TRACT
THE LIVER
THE KIDNEYS
THE ADRENAL GLANDS
THE PELVIS
INTERVENTIONAL COMPUTED TOMOGRAPHY

DENNIS L. PARKER, Ph.D.
Associate Professor, Medical Informatics; Adjunct Associate Professor, Department of Radiology; Adjunct Associate Professor, Department of Bioengineering; University of Utah School of Medicine; Associate Professor, LDS Hospital; Salt Lake City, UT
PRINCIPLES OF COMPUTED TOMOGRAPHY

RANDALL M. PATTEN, M.D.
Assistant Professor of Radiology, University of Washington School of Medicine, Seattle, WA; Medical Director, Rainier Medical Imaging Center, Kirkland, WA
THE RETROPERITONEUM AND LYMPHOVASCULAR STRUCTURES

LESLIE M. SCOUTT, M.D.
Assistant Professor, Yale University School of Medicine; Attending Radiologist, Yale-New Haven Hospital; New Haven, CT
THE PELVIS

WILLIAM P. SHUMAN, M.D.
Professor, University of Washington Medical School; Director, CT/MR, University of Washington Medical Center; Seattle, WA
THE ADRENAL GLANDS
THE RETROPERITONEUM AND LYMPHOVASCULAR STRUCTURES

RUEDI F. THOENI, M.D.
Associate Professor of Radiology, Department of Radiology, University of California, San Francisco School of Medicine; Chief, Section CT/GI, Medical Center at the University of California, Long-Moffitt Hospital, San Francisco, CA
THE GASTROINTESTINAL TRACT

EDWARD WEINBERGER, M.D.
Assistant Professor of Radiology and Adjunct Assistant Professor of Pediatrics, University of Washington School of Medicine; Children's Hospital and Medical Center; University Hospital; Seattle, WA
PEDIATRIC BODY IMAGING

PREFACE

The second edition of *Computed Tomography of the Body* has been extensively updated and is presented as a comprehensive, state-of-the-art text on computed tomography (CT) of the body that now includes an integration of magnetic resonance (MR) imaging in all sections of the book. Since the first edition, there have been great advances in CT and its application to patient care. Although the impact of CT has been enormous, magnetic resonance imaging is undergoing explosive growth and is having an ever-increasing impact on body imaging.

As in the first edition, this text is organized so that basic anatomy and CT and MR techniques are discussed for each region of the body. The features of disease entities in these two imaging modalities are described and illustrated, and the relationship of CT to MR and other imaging techniques is discussed in depth. Recommendations are offered as to the role of each modality in specific clinical situations. The book presents an integrated approach, reflecting our current standard of practice. Knowledge of CT and MR imaging will continue to expand, and recommendations, techniques, and patterns of use will undoubtedly change in the future.

In writing this book, now expanded to three volumes, there have been many people without whose support, guidance, insight, and help this work could not have been completed. We thank our colleagues who contributed their time and case material, and we acknowledge the illustration departments at the University of California, San Francisco, and the University of Washington, as well as the secretarial and editorial support of Jan Taylor, Isabel Rosenthal, and Denice Nakano.

ALBERT A. MOSS, M.D.
GORDON GAMSU, M.D.
HARRY K. GENANT, M.D.

INTRODUCTION TO VOLUME THREE

Owing to the rapid expansion of computed tomography and magnetic resonance imaging of the abdomen and pelvis, *Computed Tomography of the Body* has been expanded to three volumes, and magnetic resonance imaging has been completely integrated. Volume Three, Abdomen and Pelvis is designed as a comprehensive udpate and expansion of these topics in the first edition.

Since the first edition, high-resolution CT has become commonplace as has sub–3-second CT scanning. Magnetic resonance imaging has become a valuable procedure in the diagnosis of hepatic, adrenal, renal, prostate, and gynecologic abnormalities. Magnetic resonance imaging has been compared to computed tomography and where appropriate, recommendations are made as to the most rational use of each technology. Chapters on the physics of CT and MR imaging are included as are chapters on pediatric imagery and CT interventional procedures. The explosion of data on the use of CT and magnetic resonance imaging in the evaluation of liver and biliary tract abnormalities has necessitated expansion of the discussion of hepatobiliary tract disease into two new chapters, The Liver and The Biliary Tract.

I would like to thank the many who have helped to write this volume. In particular, I would like to thank my former colleagues at the University of California in San Francisco, my current colleagues at the University of Washington, and those from other institutions who have contributed their expertise. I would also like to thank the residents, fellows, and technicians at the University of Washington who have contributed so much to this volume. Finally, I would like to offer thanks to my secretary, Jan Taylor, for her secretarial and editorial support and to my former professors John Amberg, Richard Greenspan, Henry Goldberg, and Alexander R. Margulis.

ALBERT A. MOSS, M.D.

CONTENTS

Volume One
Thorax and Neck

CHAPTER 1
THE TRACHEA AND CENTRAL BRONCHI 1
Gordon Gamsu

CHAPTER 2
THE MEDIASTINUM 43
Gordon Gamsu

CHAPTER 3
THE PULMONARY HILA 119
Gordon Gamsu

CHAPTER 4
THE LUNGS 157
Gordon Gamsu

CHAPTER 5
THE CHEST WALL, AXILLARY SPACE,
PLEURAE, AND DIAPHRAGM 237
W. Richard Webb ▪ Gordon Gamsu

CHAPTER 6
THE HEART AND PERICARDIUM 285
Charles B. Higgins

CHAPTER 7
TRAUMA 311
Pierre Schnyder ▪ Gordon Gamsu ▪ Axel Essinger ▪ Bertrand Duvoisin

CHAPTER 8
INTERVENTIONAL TECHNIQUES 325
Jeffrey S. Klein

CHAPTER 9
THE LARYNX AND PIRIFORM SINUSES 343
Gordon Gamsu

CHAPTER 10
THE NECK 395
William P. Dillon ▪ Anthony A. Mancuso

Volume Two
Bone and Joint

CHAPTER 11
THE JOINTS 435
David W. Stoller ▪ Harry K. Genant

CHAPTER 12
THE SPINE 477
Neil I. Chafetz ▪ Stephen L. G. Rothman ▪ Harry K. Genant ▪ Jay A. Kaiser

CHAPTER 13
OSTEOPOROSIS 523
Harry K. Genant ▪ Claus-C. Glüer ▪ Peter Steiger ▪ Kenneth G. Faulkner

CHAPTER 14
MUSCULOSKELETAL TUMORS 551
Lynne S. Steinbach ▪ Harry K. Genant ▪ Clyde A. Helms

CHAPTER 15
MARROW-INFILTRATING DISORDERS 603
Bruce A. Porter

Volume Three
Abdomen and Pelvis

CHAPTER 16
THE GASTROINTESTINAL TRACT 643
Ruedi F. Thoeni ▪ Albert A. Moss

CHAPTER 17
THE LIVER 735
Richard L. Baron ▪ Patrick C. Freeny ▪ Albert A. Moss

CHAPTER 18
THE BILIARY TRACT 823
Richard L. Baron

CHAPTER 19
THE PANCREAS 869
Michael P. Federle ▪ Henry I. Goldberg

CHAPTER 20
THE KIDNEYS 933
Albert A. Moss ▪ William H. Bush

CHAPTER 21
THE ADRENAL GLANDS 1021
William P. Shuman ▪ Albert A. Moss

CHAPTER 22
THE SPLEEN 1059
Michael P. Federle

CHAPTER 23
THE RETROPERITONEUM AND
LYMPHOVASCULAR STRUCTURES 1091
Randall M. Patten ▪ William P. Shuman ▪ R. Brooke Jeffrey, Jr.

CHAPTER 24
THE PERITONEAL CAVITY AND MESENTERY .. 1139
R. Brooke Jeffrey, Jr.

CHAPTER 25
THE PELVIS 1183
Leslie M. Scoutt ▪ Shirley M. McCarthy ▪ Albert A. Moss

CHAPTER 26
PEDIATRIC BODY IMAGING 1267
Edward Weinberger ▪ David K. Brewer

CHAPTER 27
INTERVENTIONAL COMPUTED
TOMOGRAPHY 1297
Albert A. Moss

CHAPTER 28
PRINCIPLES OF MAGNETIC RESONANCE
IMAGING 1341
Peter L. Davis

CHAPTER 29
PRINCIPLES OF COMPUTED TOMOGRAPHY . 1355
Douglas P. Boyd ▪ Dennis L. Parker ▪ Mitchell M. Goodsitt

INDEX i

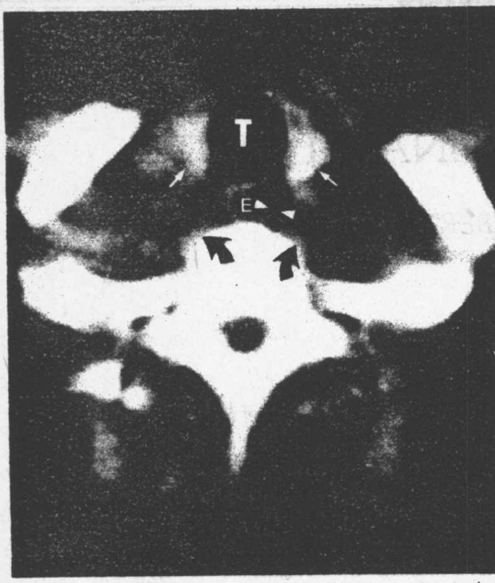

FIGURE 16–1 ■ Normal esophagus, cervical region. Cervical esophagus (E) at level of thyroid gland *(white arrows)* is positioned in the midline, just posterior to the trachea (T). The normal esophageal wall *(arrowheads)* is a thin, sharp structure outlined by air and mediastinal fat and measuring less than 3 mm in diameter. Longus colli muscles are indicated by black arrows.

esophagus is intimately related to a variety of vital vascular, pulmonary, cardiac, lymphatic, and neural structures. The esophagus is surrounded throughout most of its length by periesophageal fat that permits ready differentiation of the esophagus from adjacent structures.

The thickness of the normal esophageal wall as measured by CT in a well-distended esophagus is usually less than 3 mm (Fig. 16–1),[11, 12] and any measurement of more than 5 mm should be considered abnormal.[11, 13] Air in the esophagus is present in 40 to 60 per cent of patients examined by CT[11, 14, 15] and should not be considered an abnormal finding. Air, when present in the normal esophagus, is centrally positioned, and an eccentric position of gas within the esophagus should raise the possibility of an esophageal abnormality.[11, 14]

Upper Esophagus

The cervical esophagus is a midline structure intimately related to the posterior tracheal wall, indenting it in approximately 40 per cent of cases (see Fig. 16–1). A smooth, rounded esophageal impression on the trachea should not be interpreted as evidence of tracheal invasion by an esophageal mass. Lateral and dorsal to the esophagus on either side are the long muscles (longus colli) of the neck. The thyroid gland is seen as a high-density structure lying anterior and lateral to the trachea and esophagus. Air is present within the cervical esophagus more frequently than in any other part of the esophagus.

Middle Esophagus

At the level just below the sternal notch, the trachea deviates slightly to the right of the esophagus, with the esophagus remaining midline or shifting slightly to the left (Fig. 16–2).[11] The esophagus is closely applied to the thoracic spine, and no normal structure is found posterior to the esophagus at this level. A retrotracheal space of up to 4 mm can be present between the trachea and esophagus,[11] and a portion of lung can extend retrotracheally. The subclavian artery, common carotid artery, brachiocephalic artery, and brachiocephalic veins are also clearly identified at this level.

At the level of the aortic arch, the esophagus is closely related to the left posterolateral portion of the trachea (Fig. 16–3). The azygos vein is located to the

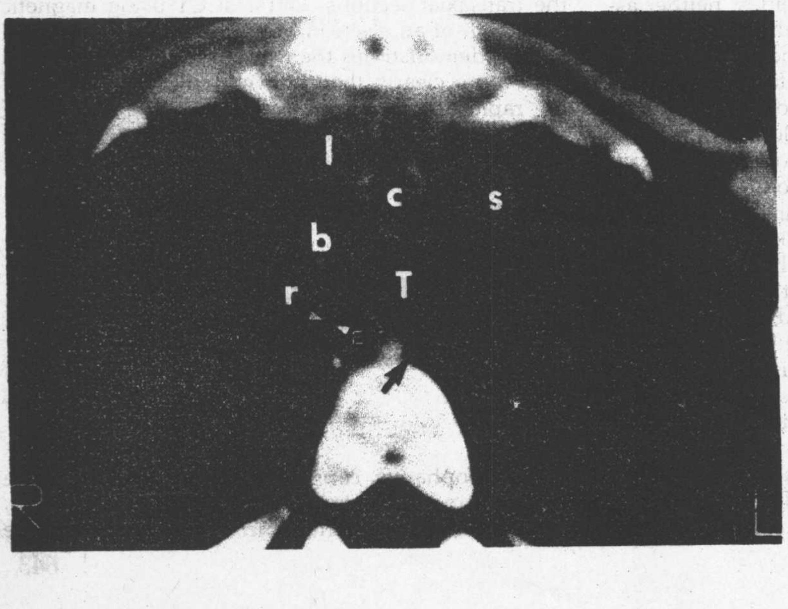

FIGURE 16–2 ■ Normal esophagus, level of sternal notch. In this patient the trachea (T) is slightly to the left of the esophagus (E). The retrotracheal extension of lung *(arrow)* is a normal finding. The left subclavian artery (s), common carotid artery (c), brachiocephalic artery (b), right (r) and left (l) brachiocephalic veins, and thin wall of the normal esophagus *(arrowheads)* are clearly identified.

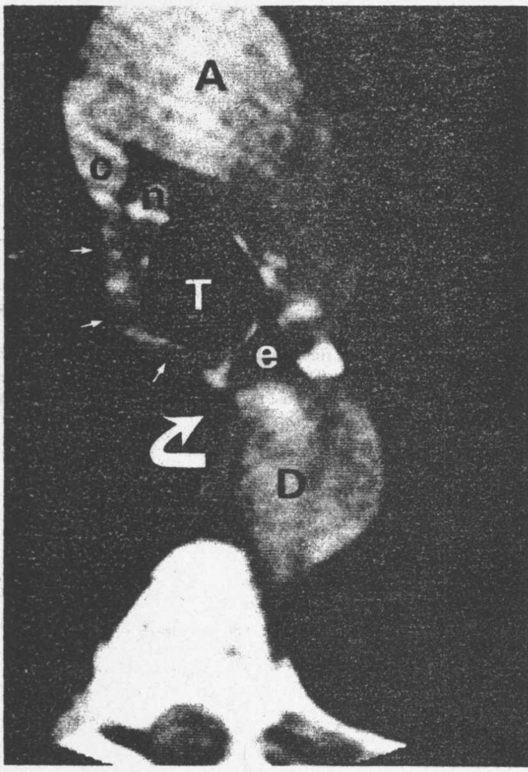

FIGURE 16–3 ■ Normal esophagus, level of aortic arch. The esophagus (e) is slightly to the right of the trachea (T), and the ascending (A) and descending (D) aorta, arch of the azygos vein *(straight arrows)* entering the superior vena cava (c) and azygoesophageal recess *(curved arrow)* are identified at this level. n = Normal-sized pretracheal lymph node.

right, posterior and lateral to the esophagus, and the arch of the azygos can be identified at this level (see Fig. 16–3). The lung is in direct contact with the right side of the esophagus, forming the azygoesophageal recess.[14] Just below the carina, the esophagus is closely related to the left main stem bronchus, separated only by a small amount of mediastinal fat (Fig. 16–4).[11, 14] At this level, a lung recess is present in 10 per cent to 20 per cent of patients between the esophagus and the left pulmonary artery.[14]

LOWER ESOPHAGUS

Below the left main stem bronchus, the esophagus comes in contact with the pericardium surrounding the posterior wall of the left atrium and is positioned near the left pulmonary vein as it enters into the left atrium. At this level the azygos vein is visible as a midline structure (Fig. 16–5). Below the level of the left atrium, the esophagus moves slightly to the left of midline just anterior to the descending aorta (Fig. 16–6), with only mediastinal fat separating the esophagus from the pericardium.

Just after the esophagus passes through the diaphragm, it turns left and courses in a horizontal plane to enter the gastric fundus (Fig. 16–7). On CT scans, the region of the gastroesophageal junction appears as a thickening along the medial cephalic aspect of the stomach in approximately one third of patients.[11, 16, 17] The apparent mass is produced as a result of the transverse plane's of axial CT sections passing through the horizontally directed normal esophagogastric junction (see Fig. 16–7).

Knowledge of the anatomy of the esophagogastric region usually permits a distinction of a true mass from a normal gastroesophageal junction. The gastrohepatic ligament courses between the lesser curvature of the stomach and liver, and the distal esophagus is enveloped by the cranialmost aspect of the ligament (Fig. 16–8).[16] The gastrohepatic ligament fuses with the fissure of the ligamentum venosum to pass anterior to the caudate lobe. Thus the cleft seen on transverse CT images separating the caudate lobe from the lateral segment of the left lobe points directly to the region of the esophagogastric junction (see Fig. 16–7).[16]

When a soft tissue mass is noted high along the lesser curvature of the stomach, its relation to the fissure plane anterior to the caudate lobe should be studied. If the mass and fissure plane are present on

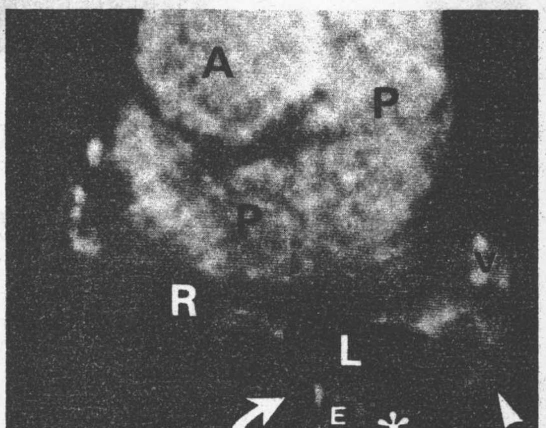

FIGURE 16–4 ■ Normal esophagus, level just below carina. A scan at this level demonstrates the relationships of the right (R) and left (L) main stem bronchi, esophagus (E), descending aorta (D), azygos vein *(straight arrow)*, pulmonary artery (P), ascending aorta (A), and azygoesophageal recess *(curved arrow)*. The left lung recess *(asterisk)* is shown abutting on the left main stem bronchus, esophagus, and left pulmonary artery *(arrowhead)*. V = Left pulmonary vein.

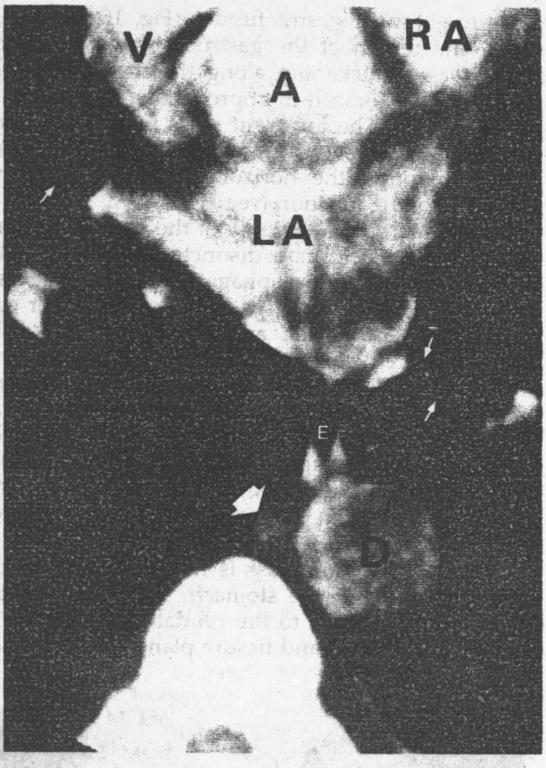

FIGURE 16–5 ■ Normal esophagus, level of left atrium. The esophagus (E) is in contact with pericardium surrounding the left atrium (LA). Pulmonary veins *(small arrows)*, right ventricle (V), right atrium (RA), ascending aorta (A), descending aorta (D), and azygos vein *(large arrow)* are also seen. At this level the esophagus is separated from lung by only the thickness of the esophageal wall and pleura.

FIGURE 16–6 ■ Normal esophagus, level of left ventricle. The esophagus (E) is just to the left of midline, closely related to the left ventricle (LV) and separated from the descending aorta (D) by the posterior junction line *(arrow)*. RV = Right ventricle; V = inferior vena cava.

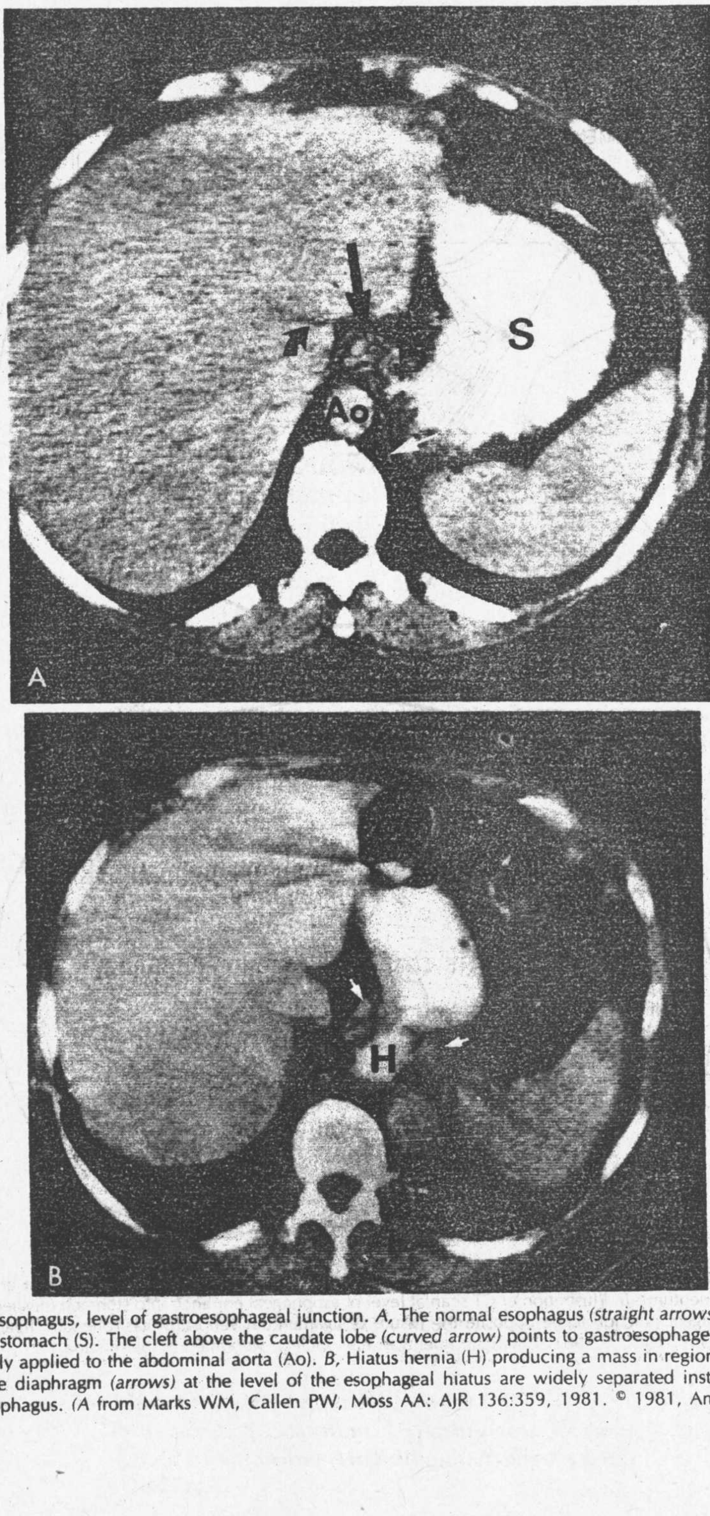

FIGURE 16–7 ■ Normal esophagus, level of gastroesophageal junction. *A,* The normal esophagus *(straight arrows)* courses in a horizontal plane to enter the fundus of the stomach (S). The cleft above the caudate lobe *(curved arrow)* points to gastroesophageal junction. Left diaphragmatic crus *(small arrow)* is closely applied to the abdominal aorta (Ao). *B,* Hiatus hernia (H) producing a mass in region of gastroesophageal junction. Note that the crura of the diaphragm *(arrows)* at the level of the esophageal hiatus are widely separated instead of tightly surrounding the descending aorta and esophagus. *(A* from Marks WM, Callen PW, Moss AA: AJR 136:359, 1981. © 1981, American Roentgen Ray Society. Reprinted by permission.)

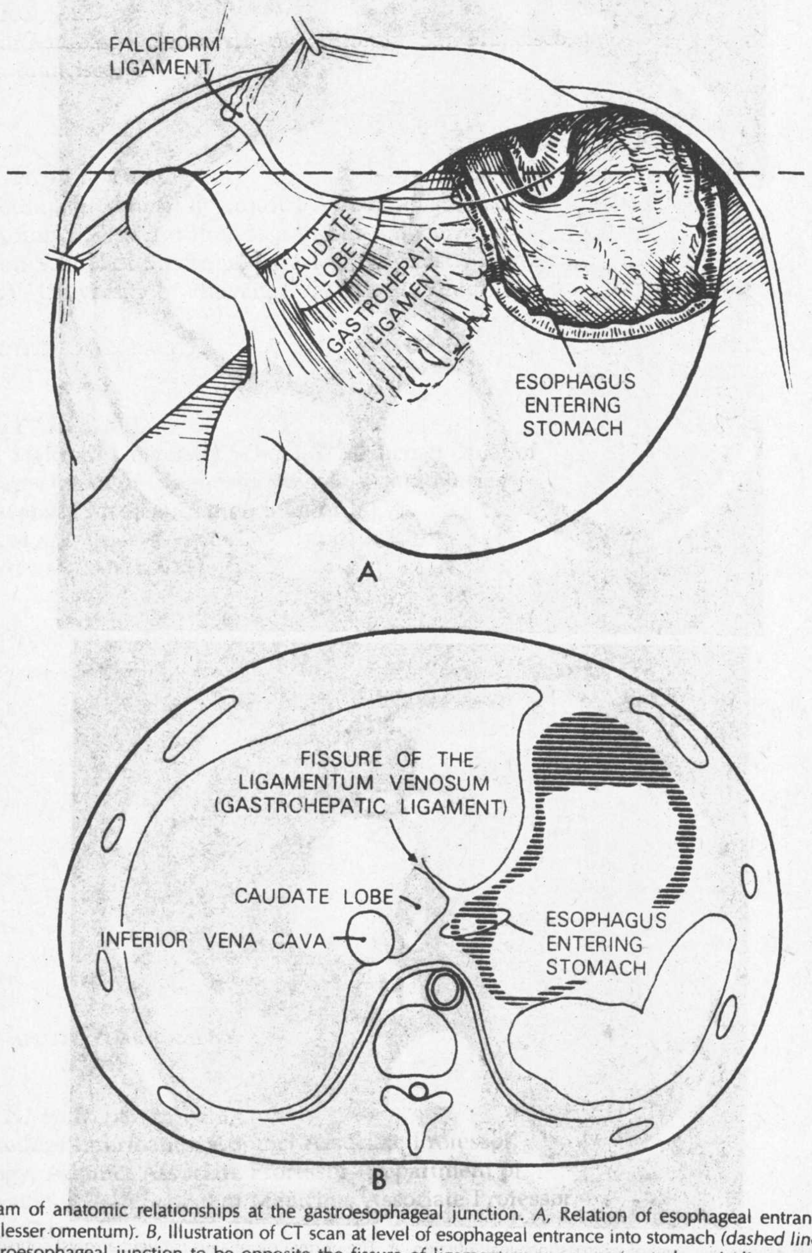

FIGURE 16–8 ■ Diagram of anatomic relationships at the gastroesophageal junction. *A,* Relation of esophageal entrance into stomach and gastrohepatic ligament (lesser omentum). *B,* Illustration of CT scan at level of esophageal entrance into stomach (*dashed line* in *A*) demonstrating the location of the gastroesophageal junction to be opposite the fissure of ligamentum venosum (gastrohepatic ligament). (From Marks WM, Callen PW, Moss AA: AJR 136:359, 1981. © 1981, American Roentgen Ray Society. Reprinted by permission.)

the same or adjoining sections, a pseudotumor should be suspected.

Techniques of Examination

Patients are routinely fasted, except for water by mouth, from midnight until the CT examination in the morning. CT scans 1 cm in thickness are taken contiguously at 1-cm intervals from the sternal notch to the umbilicus, with the patient in the supine position. The examination is extended to the umbilicus to detect abdominal lymphadenopathy, commonly found in esophageal carcinoma. CT scans of the neck are obtained if barium esophagography or endoscopy suggests a cervical esophageal lesion. Scans are obtained using the shortest available scan time with the scanner gantry at 0° angulation. CT sections thinner than 1 cm are routinely employed through areas of esophageal abnormality to better define the relationship of the esophagus to adjacent structures. In certain instances, placement of a nasogastric tube or decubitus positioning is employed to evaluate the esophagogastric junction more accurately.

An intravenous bolus of 150 to 180 mL of 60 per cent methylglucamine diatrizoate or a nonionic contrast material (iopamidol or iohexol) is administered during the scanning procedure to define the mediastinal vascular structures. Patients are not routinely given oral contrast medium to drink, but in some patients additional CT scans are obtained during or immediately following a swallow of a 1 per cent to 2 per cent solution of diatrizoate meglumine (Gastrografin) or barium sulfate in order to identify the esophageal lumen or distend the esophagus.[18, 19]

CT scans of the cervical esophagus are reconstructed using the infant or cranial reconstruction file, and the rest of the esophagus is displayed on the appropriate adult whole-body reconstruction file. The CT images of the esophagus and adjacent mediastinal structures can be magnified 1.5 to 2.5 times prior to filming to ensure optimal display of the esophagus and paraesophageal tissues.

Pathology

MALIGNANT ESOPHAGEAL TUMORS

Malignant esophageal tumors outnumber benign tumors by more than 4 to 1.[20] The majority of malignant esophageal tumors are squamous cell carcinomas, although there are scattered examples of primary esophageal adenocarcinoma, carcinosarcoma, lymphoma, sarcoma, and melanoma.[21–24] Carcinoma of the esophagus is rarely diagnosed prior to extraesophageal spread to the mediastinum, abdomen, or liver.[21–23, 25] As a result of the usually advanced state of the disease at the time of diagnosis, the overall 5-year survival rate has remained between 4 and 10 per cent,[21, 23, 26–36] despite more aggressive surgical and radiation therapy regimens. With the esophagus lacking a serosa, esophageal carcinoma can spread rapidly by way of lymphatic channels to regional lymph nodes and directly to contiguous structures such as the trachea, bronchi, and pericardium.[21, 22, 28, 29, 37]

TABLE 16–1 ■ CT Staging of Esophageal Carcinoma

Stage I	Intraluminal polypoid mass or localized thickening of esophageal wall (3 to 5 mm); no mediastinal extension or metastases.
Stage II	Thickened esophageal wall (> 5 mm) without invasion of adjacent organs or distant metastases.
Stage III	Thickened esophageal wall with direct extension into surrounding tissue; local or regional mediastinal adenopathy may or may not be present; no distant metastases.
Stage IV	Any tumor stage with distant metastatic disease.

An accurate diagnosis of esophageal carcinoma is made in more than 90 per cent of patients by esophagography or endoscopy. Chest radiography, mediastinal tomography, azygous venography, mediastinoscopy, and bronchoscopy have been used to assess the extent of disease,[37–42] although they have not proved accurate in staging carcinoma of the esophagus.[21, 22, 37, 43] Because CT accurately displays the anatomy and relationships between the esophagus and mediastinal structures,[11–15, 44–46] it has become the imaging procedure of choice to assess the degree of the spread of carcinoma into extraesophageal tissues and to determine the effect of therapy.[12, 13, 44]

CT Staging ■ Based on the CT findings, esophageal carcinoma can be classified into one of four stages (Table 16–1):

1. *Stage I:* esophageal carcinoma produces an intraluminal mass or localized esophageal wall thickening measuring 3 to 5 mm without mediastinal extension or distant metastasis. (The normal esophageal wall measures <3 mm in thickness.)
2. *Stage II:* esophageal malignancy thickens the esophageal wall to greater than 5 mm, but there is no evidence of metastatic disease or mediastinal tumor extension (Fig. 16–9).
3. *Stage III:* carcinoma thickens the esophageal wall to more than 5 mm and extends directly into the surrounding tissue (Fig. 16–10). Local or regional mediastinal lymphadenopathy may be present, but distant metastases are not seen.
4. *Stage IV:* there is evidence of distant metastatic spread with esophageal carcinoma (Fig. 16–11).

Differentiating among an esophageal squamous cell carcinoma and less frequent adenocarcinoma, melanoma, sarcoma, or mesenchymoma[47] on the basis of CT findings alone is usually not possible. Squamous cell carcinoma and esophageal adenocarcinoma are solid lesions without calcification that have a CT number close to or identical with that of adjacent soft tissues. All other esophageal malignancies except liposarcomas (Fig. 16–12), which can have a CT attenuation value close to that of periesophageal fat, also appear similar to squamous cell carcinoma of the esophagus. The administration of intravenous contrast material has not aided in differentiating